A large-area, flexible pressure sensor matrix with organic field-effect transistors for artificial skin applications

Takao Someya*†, Tsuyoshi Sekitani*, Shingo Iba*, Yusaku Kato*, Hiroshi Kawaguchi‡, and Takayasu Sakurai‡

*Quantum-Phase Electronics Center, School of Engineering, University of Tokyo, Tokyo 113-8656, Japan; and ‡Center of Collaborative Research, University of Tokyo, Tokyo 153-8904, Japan

Edited by George M. Whitesides, Harvard University, Cambridge, MA, and approved May 25, 2004 (received for review March 18, 2004)

It is now widely accepted that skin sensitivity will be very important for future robots used by humans in daily life for housekeeping and entertainment purposes. Despite this fact, relatively little progress has been made in the field of pressure recognition compared to the areas of sight and voice recognition, mainly because good artificial ''electronic skin'' with a large area and mechanical flexibility is not yet available. The fabrication of a sensitive skin consisting of thousands of pressure sensors would require a flexible switching matrix that cannot be realized with present silicon-based electronics. Organic field-effect transistors can substitute for such conventional electronics because organic circuits are inherently flexible and potentially ultralow in cost even for a large area. Thus, integration of organic transistors and rubber pressure sensors, both of which can be produced by low-cost processing technology such as large-area printing technology, will provide an ideal solution to realize a practical artificial skin, whose feasibility has been demonstrated in this paper. Pressure images have been taken by flexible active matrix drivers with organic transistors whose mobility reaches as high as 1.4 $cm^2/V{\cdot}s$. The device is electrically functional even when it is wrapped around a cylindrical bar with a 2-mm radius.

Recognition of tactile information will be very important for future generations of robots used by humans in daily life for housekeeping and entertainment purposes (1, 2). An important step to obtain good artificial ''electronic skin'' is to fabricate large-area pressure sensors with mechanical flexibility. Despite this fact, relatively little progress has been made in the field of pressure recognition compared to the areas of sight and voice recognition (1, 2). Even though flexible materials such as polymers and rubbers have been used to make sensing components, the fabrication of a sensitive skin consisting of thousands of pressure sensors would also require a flexible switching matrix that cannot be realized with present-day silicon-based electronics.

Organic field-effect transistors (3–13) are inherently flexible and very inexpensive to fabricate even for large areas (9, 10), and hence are adequate for use as a switching matrix in a pressure sensor. The minimum bending diameter reported so far, however, has been only 30 mm (11) because inorganic materials were still used in many previous transistors for some components such as gate insulators (SiO_2, Al_2O_3) and base films (glass, silicon). Moreover, the highest mobilities reported so far for plastic transistors have been around 0.1 $cm^2/V{\cdot}s$ (5), much lower than the best values around 2–5 $cm^2/V{\cdot}s$ obtained with hard substrates (13). The above two points have been major hurdles to the application of organic transistors to large-area flexible electronics.

In this article, we demonstrate an application of organic transistors in which all of the materials are soft except the electrodes. The organic transistors are integrated with a graphite-containing rubber pressure sensor layer to form a very wide area structure providing an ideal solution to realize artificial skin with low-cost processing technology. The device is illustrated in Fig. 1 and is electrically functional even when it is wrapped around a cylindrical bar with a 2-mm radius. The mobility of the organic transistors reaches values as high as 1.4 $cm^2/V{\cdot}s$, which is comparable to amorphous silicon on glass ($\approx$1 $cm^2/V{\cdot}s$) (14) and beyond values obtained on plastic films (0.4–0.6 $cm^2/V{\cdot}s$) (15, 16). The maximum effective device area is 8×8 cm^2 and contains a 32×32 array of pressure sensors. The periodicity is 2.54 mm, which corresponds to 10 dots per inch (dpi).

Device Fabrication

The manufacturing process is shown in Fig. 2*A–D*. The base film (substrate) is an ultra-high heat-resistant poly(ethylene naphthalate) (PEN) film with a thickness of 100 μm (Teonex, Q83 and Q65 from Teijin DuPont Films, Gitu, Japan).

The first step (Fig. 2*A*) is to drill holes through the base film. The laser-drilling process of polyimide sometimes results in holes with poor edge geometry, which causes poor yield of organic transistors. To avoid this problem, we first sandwiched the base film between two poly(ethylene terephthalate) (PET) films by a pouch laminator, then laser-drilled holes, and finally removed the two PET films with an organic solvent.

Then both sides are coated with 150-nm-thick gold layers with 5-nm-thick chromium adhesion layers in the vacuum evaporator with shadow masks. These layers are used to make an electronic connection between electrodes on the two sides of the base film; one side works as gate electrodes of transistors. For the patterning of gate electrodes, conventional photolithography is an alternative to use of shadow masks. Our experience is, however, that residual materials sticking to the base film during photolithography often degrade transistor performance, particularly off current. Thus we prefer to manufacture the entire device with minimum exposure to chemical solvents or water.

In the second step (Fig. 2*B*), polyimide precursors (Kemitite CT4112A, Kyocera Chemical, Kawasaki, Japan) are spin-coated and cured at 180°C to form 500-nm-thick gate dielectric layers (17). Then spots of polyimide gate dielectric layers are removed by laser drilling to make contact via holes.

A 50-nm-thick pentacene layer is deposited to form a channel layer (13, 18, 19) in the third step (Fig. 2*C*), and a 50-nm-thick gold layer is evaporated through shadow masks to form the source and drain electrodes of the transistors. The channel length L and width W are 120 μm and 2.8 mm, respectively. To prevent mechanical damage to the transistors during mechanical testing, a poly(dimethyl siloxane) (PDMS)-coated poly(ethylene terephthalate) film (not shown in Fig. 2) was also laminated.

This paper was submitted directly (Track II) to the PNAS office.

Abbreviation: SENCEL, sensor cell.

†To whom correspondence should be addressed at: Quantum-Phase Electronics Center, School of Engineering, University of Tokyo, 7-3-1 Hongo, Bunkyo-ku, Tokyo 113-8656, Japan. E-mail: someya@ap.t.u-tokyo.ac.jp.

www.pnas.org/cgi/doi/10.1073/pnas.0401918101

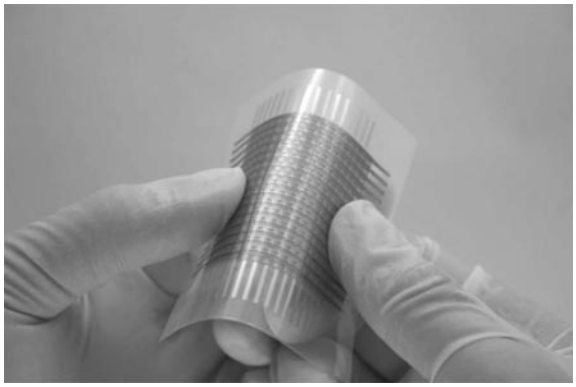

Fig. 1. Image of an electronic artificial skin. Organic transistors are used to realize a flexible active matrix, which is used to read out pressure images from the sensors. The device is bendable because all of the layers with the exception of the electrodes are made of soft materials.

In the last step (Fig. 2*D*), a pressure-sensitive rubber sheet and a copper electrode suspended by a polyimide film are laminated on the bottom of the base film to integrate pressure sensors with transistors. The pressure-sensitive flexible layer is 0.5-mm-thick PDMS containing electrically conductive graphite particles. The resistance of the rubber sheet changes when the pressure is applied on the device. Because no patterning is needed on the rubber sheet and copper electrodes, no alignment is required for this last lamination process and it would be very inexpensive to implement on a large scale. Fig. 2 *E* and *F* are top views of the entire device and of a single sensor cell (SENCEL), respectively.

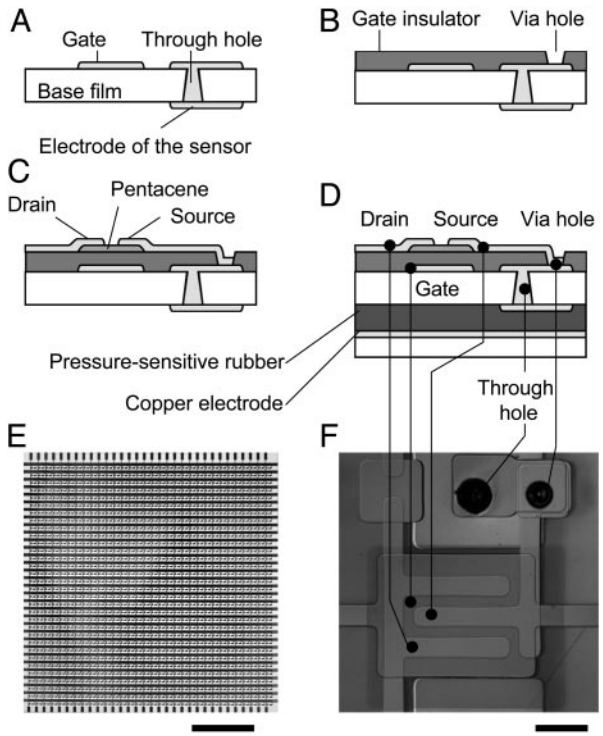

Fig. 2. Manufacturing process flow. (*A*) Through holes are drilled through a poly(ethylene naphthalate) (PEN) base film by a CO_2 laser drill machine. Then both sides of the base film are coated by 150-nm-thick gold with 5-nm-thick chromium adhesion layers in the vacuum evaporator with shadow masks. One side of the gold layer is also used as the gate electrodes of organic transistors. (*B*) A 500-nm-thick polyimide layer is prepared by spin coating as a gate dielectric layer. Then some areas of the polyimide layer are removed by the CO_2 laser drill machine to make contact via holes. (*C*) A 50-nm-thick pentacene layer is deposited in the vacuum sublimation system. Then a 50-nm-thick gold layer is deposited through a shadow mask for the source and drain electrodes. (*D*) A pressure-sensitive rubber sheet and a copper electrode suspended by a polyimide film are laminated to the bottom of the PEN film with the transistors. (*E*) A picture of a 32 × 32 array of sensor cells (SENCELs). The pitch is 2.54 mm. (Scale bar = 2 cm.) (*F*) A magnified image of a SENCEL (2.54 × 2.54 mm^2). (Scale bar = 0.5 mm.)

Some of the processing techniques used in the second step described above (Fig. 2*B*) are innovative and critical to fabricate high-performance organic transistors. A high-quality, pinhole-free, 500-nm-thick gate insulator made of polyimide was deposited on an ultrasmooth poly(ethylene naphthalate) film. Although polyimide is not an ordered material, the surface smoothness measured by atomic force microscopy is found to be 0.2 nm rms, resulting in the formation of a highly ordered pentacene thin film. Moreover, the contact holes were made by a CO_2 laser drill machine after the formation of the polyimide layer, and as a result the surface of the polyimide gate dielectric layer remained clean, and better device performance was achieved.

Device Performance

The characteristics of the organic transistors were measured in ambient environment before the application of the rubber pressure sensor film by using a semiconductor parameter analyzer. The manufactured pentacene transistors exhibit p-type conduction, and typical dc characteristics are shown in Fig. 3*A*. The field-effect mobility reaches values as high as 1.4 $cm^2/V{\cdot}s$ in the saturation regime when a −100-V operating bias is applied. The on/off ratio is 10^6 if the off current is defined as the minimum drain current at $V_{GS} = +40$ V, whereas it is 10^4 if the off current is measured at $V_{GS} = 0$ V. We have also obtained a result showing that the off current at $V_{GS} = 0$ V can be reduced drastically when transistors are manufactured without exposure to air.

The mobility of the present device is comparable to or slightly larger than that of amorphous silicon (≈1.0 $cm^2/V{\cdot}s$) and is, to the best of our knowledge, the highest ever reported for flexible organic transistors prepared on plastic films with polymeric gate insulators. A 100-V operation voltage is not realistic for artificial skin applications, but the device is still functioning and the mobility is still large (0.3 $cm^2/V{\cdot}s$) when a −20-V operating bias is applied. The initial yields of transistors exceed 99% and device failure occurs mainly because of leakage current through the gate dielectric layers. The measured drain current variation over the entire processed area is ±10%. We speculate that the origin of the variations should be attributed mainly to the thickness fluctuation of polyimide gate dielectric layers. Polyimide precursors do not wet easily when they are spin-coated on gold electrodes. Thus, it is important to minimize the interval between the end of spin coating and the start of baking to avoid the formation of droplets of polyimide precursors, which degrade the uniformity of the thickness of polyimide gate dielectric layers.

The complete devices including the rubber pressure sensors are characterized by applying a pressure by using a square block made of rubber to avoid scratching. The circuit diagram of an individual SENCEL is shown in the *Inset* of Fig. 3*B* and the overall configuration is similar to a memory cell and pixel of a charge-coupled device (CCD): gate electrodes of each line are connected to a word line (V_{WL}), whereas drain electrodes of each line are connected to a bit line (V_{BL}). Typical results of the measured change in the drain current (I_{DS}) dependence of the gate voltage (V_{GS}) are shown in Fig. 3*B*. As the pressure is applied on the device and varies from 0 to 30 kPa (≈300 gram force/cm^2), the resistance of the rubbery sheet varies from 10

ENGINEERING

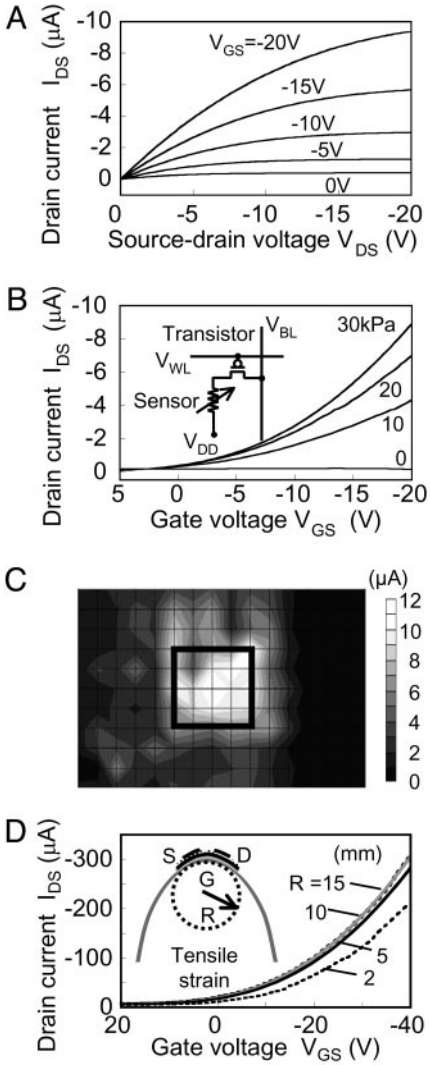

Fig. 3. Device characteristics. (*A*) Drain current (I_{DS}) measured for the transistors with pentacene as a channel layer, showing p-type conduction. The source–drain voltage (V_{DS}) is swept from 0 V to −20 V under gate bias (V_{GS}) from 0 V to −20 V with −5-V steps. (*B*) Transfer curves (I_{DS} vs. V_{GS}) are measured for a SENCEL under application of various pressures from 0 to 30 kPa. V_{DS} = −20 V is applied. The resistance of the pressure-sensitive conductive rubber changes between 10 MΩ and 1 kΩ when it is off and on. (*Inset*) The circuit diagram of each SENCEL is shown. V_{BL}, bit line; V_{WL}, word line; V_{DD}, supply voltage. (*C*) The fabricated sensor matrix is pressed with a rectangular rubber block. The position dependence of the drain current is monitored with applying voltage bias of V_{DS} = −20 V and V_{GS} = −20 V. The solid square indicates where the rubber block was positioned. (*D*) The transfer curves (I_{DS} vs. V_{GS}) are measured for a pentacene transistor rolled around cylindrical bars with various radii as schematically shown in the *Inset*. S, source; D, drain; G, gate. The channel length (*L*) and width (*W*) are 50 μm and 16 mm, respectively. The electronic performance does not change when the bending radius (*R*) is changed from 50 to 10 mm. Further reduction of *R* causes decrease of drain current I_{DS}, but the transistor is still functional even at *R* = 2 mm.

MΩ to 1 kΩ and the transconductance as well as the measured current increases.

A pressure spatial map was obtained by applying individually to each SENCEL voltages V_{DS} = −20 V for each bit line and V_{GS} = −20 V for each word line under pressure from a rubber block. Fig. 3*C* shows results of the current level obtained for each SENCEL. One of the transistor devices at the upper left corner of the square is not functioning because of a deformation of the gate layer leading to open circuits. The observed pressure gradient toward the center of the rubber block is due to its finite size, which causes a nonuniform deformation of the pressure sensor rubber layer beneath it.

To perform bending tests, individual transistors with larger channel length and width (L = 50 μm and W = 16 mm) were processed and characterized as schematically described in the *Inset* of Fig. 3*D*. The 60-μm-thick base film with organic transistors was rolled on bars with radius R varying from 50 to 2 mm, which corresponds to tensile strain from 0.1% to 1.5%, respectively, induced parallel to the current flow. I_{DS} was monitored as a function of the gate voltage V_{GS} at a drain source voltage V_{DS} = −40 V.

The magnitude of the drain current I_{DS} remains practically unchanged when the bending radius decreases from 50 to 10 mm, whereas a slight decrease by only 3% is measured for R = 5 mm. The organic transistors were still functional even with a 2-mm bending radius and the mobility was decreased by only 20%, demonstrating that we have achieved much mechanically flexibility and high mobility simultaneously for organic transistors with polyimide gate insulators. In previous related work, inorganic gate insulators such as SiO_2 and SiN and/or indium-tin oxide (ITO) gate electrodes were used and tensile failure occurred at bending diameter above 30 mm (11). In our case, bending was limited by necking of gold electrodes for radius $R \approx$ 1 mm. No significant damage or residual effect due to bending stress was observed in the devices, and the current level in the saturation regime measured in a flat position after bending down to R = 4 mm remained unchanged. However, a slight increase of the off current (I_{DS} at V_{GS} = 0 V) was observed, which is not surprising because a time-dependent drift of the threshold voltage due to air exposure was also independently observed.

For integrated devices, performance variation induced by strains is mainly due to the performance variation of transistors because the pressure sensors are made of silicone rubber, which is very resistant to strain induced by bending. When the pressure-sensitive rubber sheet is wrapped around a bar with a 10-mm radius, this strain is estimated to be 6 kPa pressure, which is below the sensitivity of pressure sensors (30 kPa), and does not influence electronic performance. We assume Poisson's ratio of 0.46 and Young's modulus of 0.3 MPa for estimation of strain effects in the silicone rubber sheet (20). The strain effects in the rubber sheet would be easily reduced by thinning its thickness.

Discussion

It should be noted that the design of the device described in this work is completely different from the one of previous pressure sensor arrays because a flexible active matrix structure is used. Readers may be aware of the development of liquid crystal displays (LCDs), which used to be operated by static or simple matrix drivers and have now evolved to an active matrix design. Similarly, the first area sensors were assembled with discrete devices, operated by static drivers and required individual wires to each cell. More recently, a simple matrix design (with no access transistors) has been used for large-area pressure sensors (21) requiring high power consumption and expensive additional driving electronics to compensate roundabout current routes or cross talks. In the active matrix driving method presented here only one transistor needs to be in an "on" state for each SENCEL where pressure is applied so that it is the only design suitable for low-power applications where a high number of SENCELs is required over large areas, such as electronic skin. Moreover, with an active matrix design the sensor array could easily become "smart" to realize functions such as a progressive scan, SENCEL skipping, and others.

It is well known that the mobility of organic semiconductors is about three orders of magnitude lower than that of silicon (22) and a major disadvantage for applications such as video-rate display (18, 23) and radio frequency (rf) identification

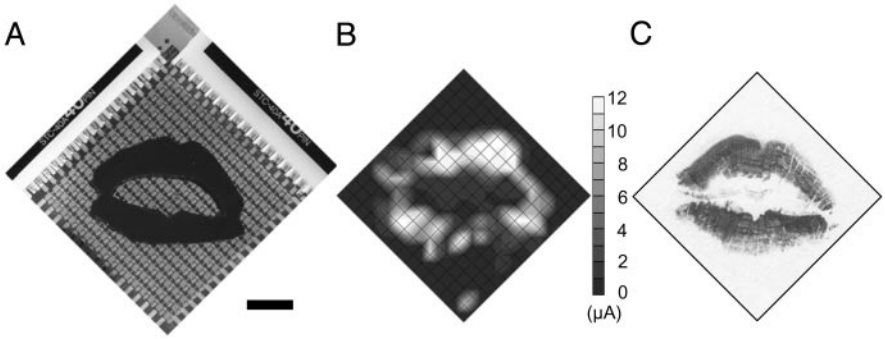

Fig. 4. A pressure image of a kiss mark is taken by using the present sensors. The device, consisting of 16 × 16 SENCELs, is pressed with a lip-shaped rubber replica (*A*) and the pressure image (*B*) is compared with the print on paper (*C*). The current of each SENCEL is measured with a −20-V operating bias. The two bright spots at the bottom of *B* are due not to a failure of transistors but to a failure of sensors around those two spots (low local resistance of the pressure-sensitive rubber). (Scale bar = 1 cm.)

tags (13, 24–26), which have been recognized so far as the main motivations for the development of organic transistors. In the case of area sensors, however, the slower speed is tolerable for most applications. For artificial skin in particular, the integration of pressure sensors and organic peripheral electronics allows one to take advantage of the many benefits of organic transistors such as mechanical flexibility, large area, low cost, and relative ease of fabrication without suffering from their drawbacks. Similar functions may be achieved by amorphous silicon on plastic films (15, 16), and the present study demonstrates the general feasibility of large-area electronics from the context of sensor applications.

The accuracy of the pressure intensity reading over large areas (pressure gradation) is limited mainly by the uniformity of the performance of organic transistors, whereas the sensitivity itself is limited by the performance of the pressure-sensitive conducting rubber. The present device can detect a few tens of kilopascals, which is comparable to the sensitivity of discrete pressure sensors. The integration of organic transistors with more sophisticated pressure sensors, such as poly(vinylidene difluoride) (PVDF)-based strain/pressure sensors or sensors with pressure-sensitive ink, would be helpful to improve the performance of artificial skin devices.

It should also be relatively straightforward to improve the density of the sensor matrix because in the manufacturing scheme used in this work, it is limited by the resolution of metal shadow masks. The pitch is 2.54 mm in the present device, which is sufficient for most artificial skin applications, but a much higher density could easily be obtained by reducing device dimensions or using a shorter channel length. The current channel length is relatively large (120 μm), leaving plenty of room for down-scaling with no major technical obstacles. The use of shadow masks with a 20-μm resolution has been reported recently for large-area organic circuits (13, 24). An increase of the SENCEL density would allow one to easily reach a high spatial resolution, and the integration of artificial sensors for other somatic senses located in the skin (temperature and humidity, for example) to better emulate real human skin would also be feasible. Furthermore, an important feature that would be desirable in artificial skin is stretching capability, because real human skin can be stretched.

The time response of the pressure-sensitive rubber is typically of the order of hundreds of milliseconds, and the individual sensor does not respond to the higher frequency. It should be noted, however, that the readout time of an entire 16 × 16 sensor cell array is *not* the response time of individual transistors multiplied by 16 × 16 because an active matrix scheme is used. The scan speed of the entire sensor cell array is limited by the performance of individual transistors and is independent of the frequency response of the pressure sensors. The cycle time of each transistor was measured to be around 30 ms in this study, from which the total time to access 16 × 16 transistors is estimated to be 480 ms if one word line is read at the same time. This total access time is comparable to the response time of the pressure sensor, so that for a larger device with a large number of sensor cells, the organic transistors will be the limiting factor of the frequency response.

One additional, playful experiment performed consisted in applying to one of the sensors we fabricated a rubber structure shaped as human lips. The image obtained by using the pressure sensor is shown in Fig. 4 along with a photograph of the "rubber lips" used to apply pressure. Even though the resolution of the present device is too low for the sensor to identify whose lips it is touching, the experience is conclusive enough to fuel one's imagination.

We thank Profs. Yasuhiko Arakawa, Hiroyuki Sakaki, Makoto Gonokami, and Tadashi Kobayashi for fruitful discussions, and Dr. Jean Benoit Héroux for critical reading of the manuscript. This study was partially supported by the New Energy and Industrial Technology Development Organization, the Ministry of Public Management, Home Affairs, Posts and Telecommunications, and the Ministry of Education, Culture, Sports, Science, and Technology Information Technology and Center-of-Excellence programs.

1. Nicholls, H. R. & Lee, M. H. (1989) *Int. J. Robotics Res.* **8,** 3–30.
2. Lee, M. H. & Nicholls, H. R. (1999) *Mechatronics* **9,** 1–31.
3. Tsumura, A., Koezuka, H. & Ando, T. (1986) *Appl. Phys. Lett.* **49,** 1210–1212.
4. Burroughes, J. H., Jones, C. A. & Friend, R. H. (1988) *Nature* **335,** 137–141.
5. Sirringhaus, H., Tessler, N. & Friend, R. H. (1998) *Science* **280,** 1741–1744.
6. Dimitrakopoulos, C. D., Purushothaman, S., Kymissis, J., Callegari, A. & Shaw, J. M. (1999) *Science* **283,** 822–824.
7. Katz, H. E., Lovinger, A. J., Johnson, J., Kloc, C., Siegrist, T., Li, W., Lin, Y.-Y. & Dodabalapur, A. (2000) *Nature* **404,** 478–481.
8. Sirringhaus, H., Kawase, T., Friend, R. H., Shimoda, T., Inbasekaran, M., Wu, W. & Woo, E. P. (2000) *Science* **290,** 2123–2126.
9. Mirkin, C. A. & Rogers, J. A. (2001) *MRS Bull.* **26,** 506–508.
10. Dimitrakopoulos, C. D. & Malenfant, P. R. L. (2002) *Adv. Mater.* **14,** 99–117.
11. Loo, Y.–L., Someya, T., Baldwin, K. W., Bao, Z., Ho, P., Dodabalapur, A., Katz, H. E. & Rogers, J. A. (2002) *Proc. Natl. Acad. Sci. USA* **99,** 10252–10256.
12. Stutzmann, N., Friend, R. H. & Sirringhaus, H. (2003) *Science* **299,** 1881–1884.
13. Kelley, T. W., Muyres, D. V., Baude, P. F., Smith, T. P. & Jones, T. D. (2003) *Mater. Res. Soc. Symp. Proc.* **771,** 169–179.
14. Kuo, Y., ed. (2004) *Thin Film Transistors: Materials and Processes* (Kluwer, Dordrecht, The Netherlands).
15. Won, S. H., Chung, J. K., Lee, C. B., Nam, H. C., Hur, J. H. & Jang, J. (2004) *J. Electrochem. Soc.* **151,** G167–G170.

16. Gleskova, H. & Wagner, S. (1999) *IEEE Electron Device Lett.* **20,** 473–475.
17. Kato, Y., Iba, S., Teramoto, R., Sekitani, T., Someya, T., Kawaguchi, H. & Sakurai, T. (2004) *Appl. Phys. Lett.* **84,** 3789–3791.
18. Klauk, H., Gundlach, D. J. & Jackson, T. N. (1999) *IEEE Electron Device Lett.* **20,** 289–291.
19. Klauk, H., Halik, M., Zschieschang, U., Schmid, G., Radlik, W. & Weber, W. (2002) *J. Appl. Phys.* **92,** 5259–5263.
20. Mark, J., ed. (1999) *Polymer Data Handbook* (Oxford Univ. Press, New York).
21. Azuma, T. (2001) *Sens. Mater.* **13,** 107.
22. Crone, B., Dodabalapur, A., Lin, Y.-Y., Filas, R. W., Bao, Z., LaDuca, A., Sarpeshkar, R., Katz, H. E. & Li, W. (2000) *Nature* **403,** 521–523.
23. Rogers, J. A., Bao, Z., Baldwin, K., Dodabalapur, A., Crone, B., Raju, V. R., Kuck, V., Katz, H., Amundson, K., Ewing, J. & Drzaic, P. (2001) *Proc. Natl. Acad. Sci. USA* **98,** 4835–4840.
24. Baude, P. F., Ender, D. A., Haase, M. A., Kelley, T. W., Muyres, D. V. & Theiss, S. D. (2003) *Appl. Phys. Lett.* **82,** 3964–3966.
25. Gelinck, G. H., Geuns, T. C. T. & de Leeuw, D. M. (2000) *Appl. Phys. Lett.* **77,** 1487–1489.
26. Drury, C. J., Mutsaers, C. M. J., Hart, C. M., Matters, M. & de Leeuw, D. M. (1998) *Appl. Phys. Lett.* **73,** 108–110.